DOI: 10.13009/EUCASS2022-4391
9TH EUROPEAN CONFERENCE FOR AERONAUTICS AND SPACE SCIENCES (EUCASS)

Experimental study to verify oil loss through the vent line of the aero-engine lubrication system

LI Lixian, DI MATTEO Mariano** and HENDRICK Patrick***
**EPF Graduate School of Engineering*
EPF École d'ingénieurs, 3 bis Rue Lakanal, 92330 Sceaux, France. lixian.li@epfedu.fr
*** Aero-Thermo-Mechanics Dept., Université Libre de Bruxelles*
Avenue F. D. Roosevelt 50, 1050 Bruxelles, Belgique. mariano.di.matteo@ulb.be, patrick.hendrick@ulb.be

Abstract
Oil leakage of the lubrication system increases the oil consumption and emissions. Moreover, leakages on the bearing chambers at compressor level may pollute the bleeding air. The aim of this research is to investigate different operating conditions (the water flow rate, the air/water volume ratio, the level of the air/water mixture in the tank, and the operating air pressure limit) in the engine oil system that could potentially increase (cause/avoid) oil leaks. The fluid used was water at 20°C instead of oil at 150°C. The results show the impact of operating conditions on the leakage.

1. Introduction

The oil system is a closed loop. At each oil circulation cycle, the oil is sent from the oil tank by a pump, after passing through the moving parts (bearing chamber, gearboxes, etc.), the oil will be returned to the tank by a recovery pump [1]. However, the oil is in contact with the air during its journey, the return oil contains a certain amount of air that must be eliminated by a degasser and be set free at the tank, this air containing a small amount of oil will be conducted to the "vent line", filtered by a breather before being vented out in the atmosphere. This leakage represents both an increase in oil consumption and a source of atmosphere pollution.

The leaks due to operating conditions are also present in the bearing chamber. The labyrinth seals are the most widely used oil sealing element in jet engines and stationary turbomachinery [2]. However, the large radial gaps at the seals imply a significant oil leakage [3]. This leakage increases the oil consumption and pollutes the cabin/cockpit air, which may cause a new occupational disease that is not yet officially recognized: the aerotoxic syndrome. Compressed air at a temperature suitable for breathing is required. At the end of the sixties, with the design of the Caravelle, aircraft were equipped with an air bleed system at the engine compressor to gain weight and efficiency. However, this air, also called "Bleed air", is taken from the engine stages, which passes through the moving parts lubricated at high temperature, there remains a small amount of lubricating oil that contains toxic components, mainly the anti-wear agent TCP [4-5]. They therefore make bleed air toxic. Aerotoxic syndrome is a disease caused by the effects of inhalation the contaminated air. This syndrome represents differently on the different individuals, the symptoms are very diverse, they can be neurotoxic, psychotoxic, gastrointestinal, respiratory, cardiovascular, irritated, etc. The main victims are the crews (especially pilots), maintenance workers, ground staff and frequent flyers because of the recurrence and long duration of their exposure. [5-8].

Many researchers have proposed solutions for oil leakage deduction from different perspectives. They mostly focused on 2 aspects, either to reduce losses in the bearing chamber by changing the type of seal, brush seal for example [3], or to reduce the emissions in the atmosphere by improving the efficiency of separators. Several theoretical models allowing to calculate the efficiency of these separators by knowing their geometry and/or by designing the geometry of the separator to obtain the desired efficiency have been proposed [10]. Leakage is reduced but still possible in both cases [11]. Our study focuses on the analysis of the impact of the operating conditions. Some models of the separator remain efficient for whatever operating conditions [12], so if we could prove that operating conditions have an impact on oil leakage, based on these improved efficiency separators, we could further prevent oil leakage by adjusting the operating conditions.

The objective of this project is to understand whether there are operating conditions in the engine oil system that could potentially cause/avoid oil leakage to evaluate the possibility of controlling the oil leak without changing the oil structure.

DOI: 10.13009/EUCASS2022-4391

2. Methodology and experimental set-up

In this part, to highlight the influences of the operating conditions of the oil system on the leakage, tests were carried out on the ATM06 test bench which simulates the operation of the oil system. We will start with a study of similarity between water at 20°C and oil at 150°C to justify our choice of fluid used, then a presentation on the test bench and ends with a discussion on the results obtained.

2.1 Similarity between water (20°C) and oil (150°C)

Lubricating oil is expensive, dirty, and corrosive. Based on the similarity between water at temperature 293.15 K (20°C) and oil at temperature 423.15 K (150°C), experiments are performed with water and air at room temperature (about 293.15 K) to simulate the real situation in the compressor from where the oil is at 423.15 K [13].

We study the similarity of these two incompressible fluids based on four characteristic numbers:
the Reynolds number which is often used to characterize the flow regime of a fluid and the similarity between fluids, it is expressed in:

$$\boldsymbol{Re = \frac{vL}{\nu}} \tag{1}$$

the Pressure coefficient which represents the pressure distribution around an obstacle in a fluid flow:

$$\boldsymbol{Cp = \frac{\Delta P}{\frac{1}{2}\rho v^2}} \tag{2}$$

the Weber number, which characterize fluid flow at the interface of a multiphase system (the flow of the oil system is a complex two-phase oil-air flow):

$$\boldsymbol{We = \frac{\rho v^2 L}{\sigma}} \tag{3}$$

the Froude number:

$$\boldsymbol{Fr = \frac{v}{\sqrt{gL}}} \tag{4}$$

With v the speed of the flow, ν the kinematic viscosity in m^2/s, L the characteristic length in m, ΔP the pressure difference between the static pressure at the measured point and that of the flow in Pa, ρ the density in kg/m^3, sigma the surface tension of the drop in N/m, g the gravity in m/s^2.

According to the definitions of these characteristic numbers, the similarity depends mainly on the viscosity ν and the density ρ with the same condition of the flow. The surface tension of water is about twice that of oil, but the surface tension can be reduced by reducing the size of the drops by spraying for example. For viscosity and density, taking the example of jet oil type 2 which is commonly used in aerospace application, according to its data sheet, the density of oil is 1003.5 kg/m^3 which is close to that of water which is 998 kg/m^3, its oil viscosity is 27.6×10^{-6} m^2/s at 313.15 K (40°C), and is 5.1×10^{-6} m^2/s at 393.15 K (100°C). The viscosity is proportional with temperature in the logarithmic scale [14], so the viscosity of oil at 423.15 K can be calculated:

$$\boldsymbol{\nu(T) = Aexp\left(\frac{\alpha}{T}\right)} \tag{5}$$

$$\boldsymbol{ln(\nu) = ln(A) + \alpha(\frac{1}{T})} \tag{6}$$

The constant coefficients A and α can be deduced with the two viscosity values at two temperatures:

DOI: 10.13009/EUCASS2022-4391

$$\alpha = \frac{ln\left(\frac{\nu_{393.15\,K}}{\nu_{313.15\,K}}\right)}{\frac{1}{T_{393.15\,K}} - \frac{1}{T_{313.15\,K}}} \tag{7}$$

$$ln(A) = ln(\nu_{313.15\,K}) - \alpha\left(\frac{1}{T_{313.15\,K}}\right) = ln(\nu_{393.15\,K}) - \alpha(\frac{1}{T_{393.15\,K}}) \tag{8}$$

$$\nu_{423.15\,K} = e^{ln\,(\nu_{423.15\,K})} = e^{ln(A)+\alpha(\frac{1}{T_{423.15\,K}})} \tag{9}$$

With the numerical application on equations (7), (8) and (9):

$$\nu_{huile_{423.15\,K}} = 1,8\,cSt = 1.8\,\times 10^{-6}\,m^2/s$$

The viscosity of oil at 150°C IS 1.8 × 10^{-6} m^2/s, compared to the viscosity of water at 20°C which is 1.0 × 10^{-6} m^2/s, and oil viscosity at 150 °C was also verified experimentally:

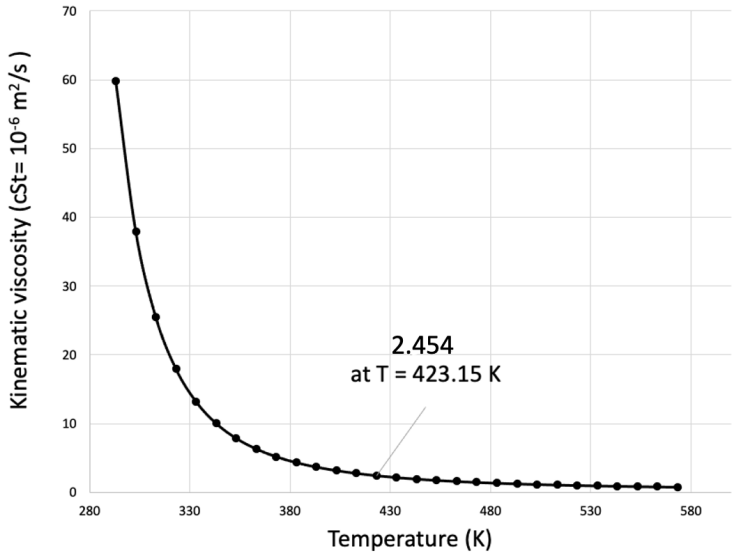

Figure 1: Evolution of the kinematic viscosity of jet oil type 2 according to temperature

The viscosity of oil is 2.454 × 10^{-6} m^2/s at 423.15 K according to the experimental data, it remains close to that of water at 293.15 K (Fig.1). Therefore, water (293.15 K) and oil (423.15 K) have a remarkable similarity, the results of the experiments with water (293.15 K) are therefore representative for the real situation.

2.2 Presentation of the test bench

The ATM06 laboratory test bench simulates the operation of the oil cycle. It is composed mainly by a water tank, two turbo pumps, a compressor, an air-water cyclone separator and a weighing scale. The bench remotely controlled by MatLab Simulink software, that allows us to retrieve the data of the measured parameters in continuous time. Table 1 shows the measured parameters. The pump sent the water in pressure to the line. The water is mixed with compressed air. The air-water mixture will be separated by the cyclone air-water separator. The water will be returned to the tank by the recovery pump. The air with a small amount of water is vented out and the leakage will be measured by the weighing scale (Fig.2).

DOI: 10.13009/EUCASS2022-4391

Table 1. Measured parameters of the bench

	Symbol	**Unit**
Water inlet flow rates	$D_{water-i}$	[m^3/h]
Air inlet flow rates	D_{air-i}	[m^3/h]
Water inlet/outlet pressure	$P_{water-i/out}$	[Pa]
Air inlet/outlet pressure	$P_{air-i/out}$	[Pa]
water-air mixture inlet/outlet pressure	$P_{water-air-i}$	[Pa]
Water inlet pressure	$T_{water-i}$	[K]
Air inlet pressure	$T_{air-i/out}$	[K]
Water-air mixture inlet/outlet pressure	$T_{water-air-i/out}$	[K]
Mixture air/water volume ratio	$r_{air/water}$	[/]

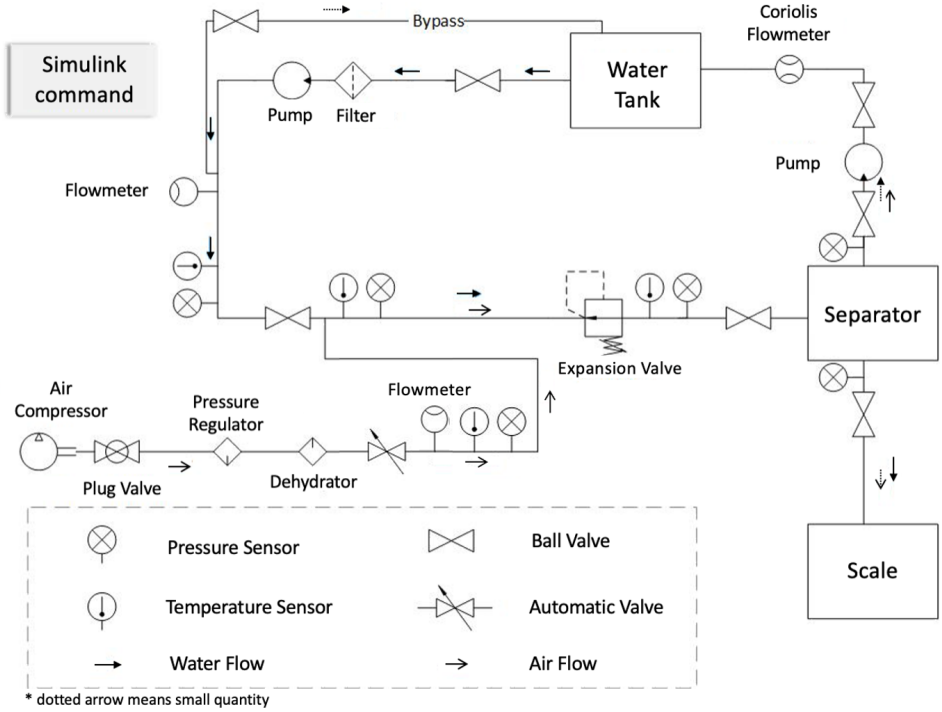

Figure 2: Schema of the test bench ATM06

The two pumps operating conditions and the air flow rates are controlled by Simulink, which also retrieves the sensor data and displays it (Fig. 3). The leakage mass of water can be read directly on the scale, and the leakage time must be timed to calculate the leakage rate of water.

DOI: 10.13009/EUCASS2022-4391

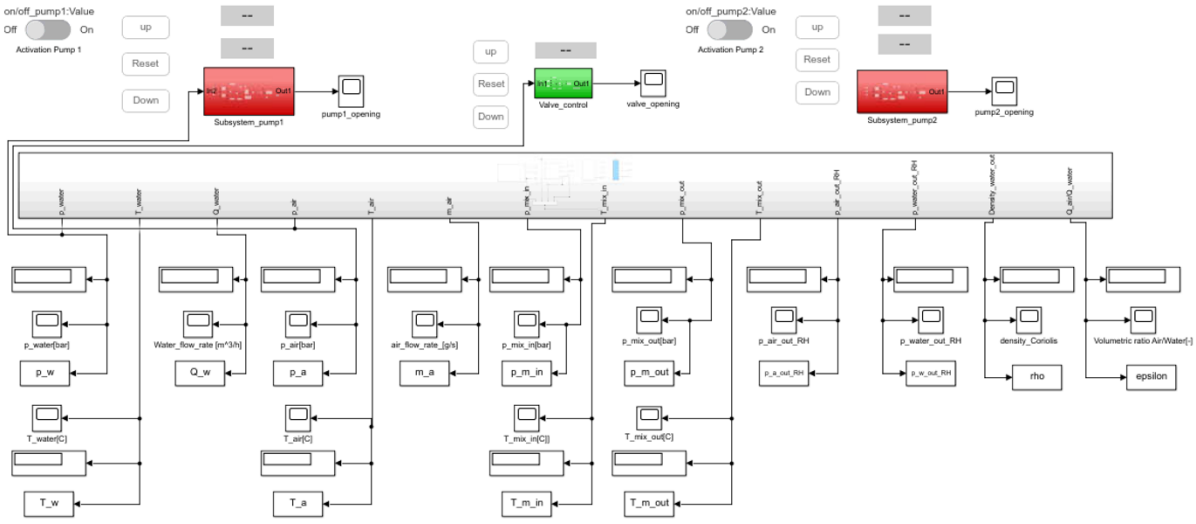

Figure 3: Command post - Simulink block

The tests were carried out for inlet water flows ($D_{water\text{-}i}$) from 3 to 9 m^3/h, the air/water volume ratios ($r_{air/water}$) from 0 to 3 and different air/water levels in the tank which is connected to the separator (h). The tests are repeated three times to verify the recurrence of the results. However, the results of these tests show that there are possible influences on the leakage by the operational pressures, so the tests for different limit pressures (P_lim) at the exit of the compressor are added.

3. Experimental results and analysis

By grouping and processing the test data, maps according to the different parameters are established by taking the average values of the three repetitions for leakage and heights. For the inlet water flows and ratios, only one significant figure is kept being able to compare between several curves. Thus, the data of each test are also presented on the maps in the form of scatter plots to have a global view on the distribution of the points around the average value.

3.1 Results according to the levels of the air/water mixture in the tank

Figures 4-8 are the maps according to the three levels of the air/water mixture h: 67.4 cm, 41 cm and 23.5 cm (the averages), for the different values of water flow rate and the different ratios. According to these results, the level of the mixture does not have a significant influence on the leakage, the deviation of the water leakage between the different levels is of the order of 0.1 g/s, but the uncertainty of reading on the balance is ± 0.01 kg, i.e., 10g, also the uncertainty for reading of chronometer is 0.1s, therefore this deviation of the order of 0.1 g/s can be neglected.

Moreover, these results show the possible presence of another parameter than water level, water flow rate and ratio air/water that may impact the water leakage. It is observed that the leakage increases with the increase of water flow rates $D_{water\text{-}i}$, but figure 5 shows that for a ratio $r_{air/water} = 1.5$, the water leakage for $D_{water\text{-}i} = 7$ m^3/h and for $D_{water\text{-}i} = 8$ m^3/h are nearly the same. Figure 6 shows the results for a ratio $r_{air/water} = 2$, at different water level inside the tank (height). We observe a nonlinear behavior, the differences between $D_{water\text{-}i} = 5$ m^3/h and $D_{water\text{-}i} = 6$ m^3/h, and between $D_{water\text{-}i} = 7$ m^3/h and $D_{water\text{-}i} = 8$ m^3/h are all about 0. 5 g/s, but the difference between $D_{water\text{-}i} = 6$ m^3/h and $D_{water\text{-}i} = 7$ m^3/h is about 2.5 g/s which is larger compared to the other. In addition, generally the higher the water flow rate at the inlet, the higher the water leakage, except that in figure 6, the leakage of the water flow rate at 5 m^3/h is higher than that at 6 m^3/h. These anomalies suggest that there is maybe another parameter that plays an important role.

DOI: 10.13009/EUCASS2022-4391

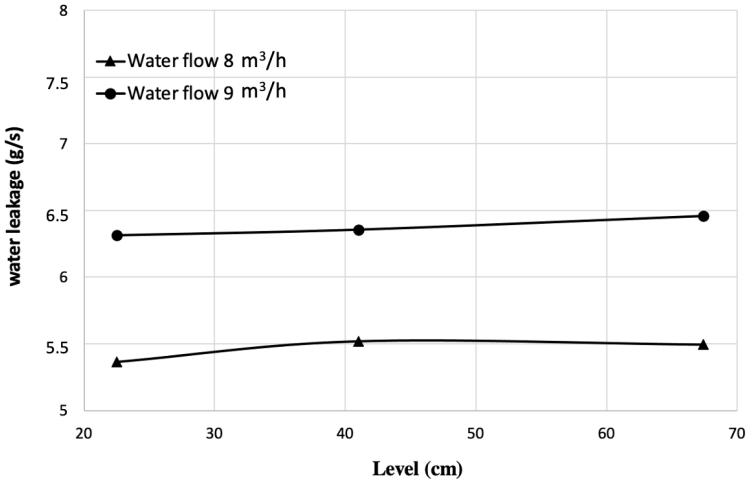

Figure 4: Leakage as a function of level for different water inlet flows ($r_{air/water}$ = 1)

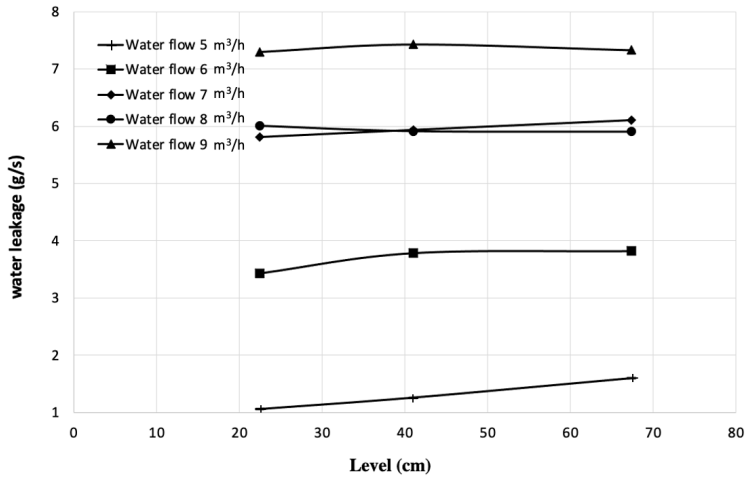

Figure 5: Leakage as a function of level for different water inlet flows ($r_{air/water}$ = 1.5)

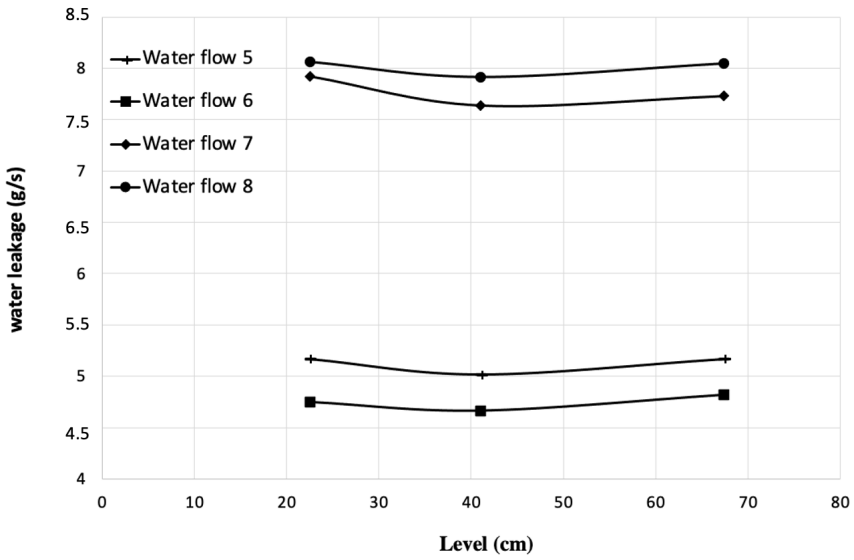

Figure 6: Leakage as a function of level for different water inlet flows ($r_{air/water}$ = 2)

DOI: 10.13009/EUCASS2022-4391

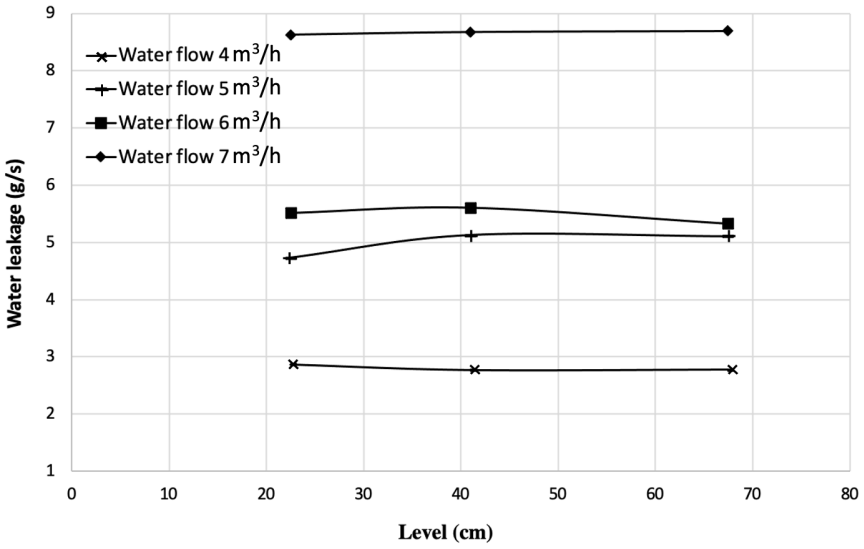

Figure 7: Leakage as a function of level for different water inlet flows ($r_{air/water}$ = 2.5)

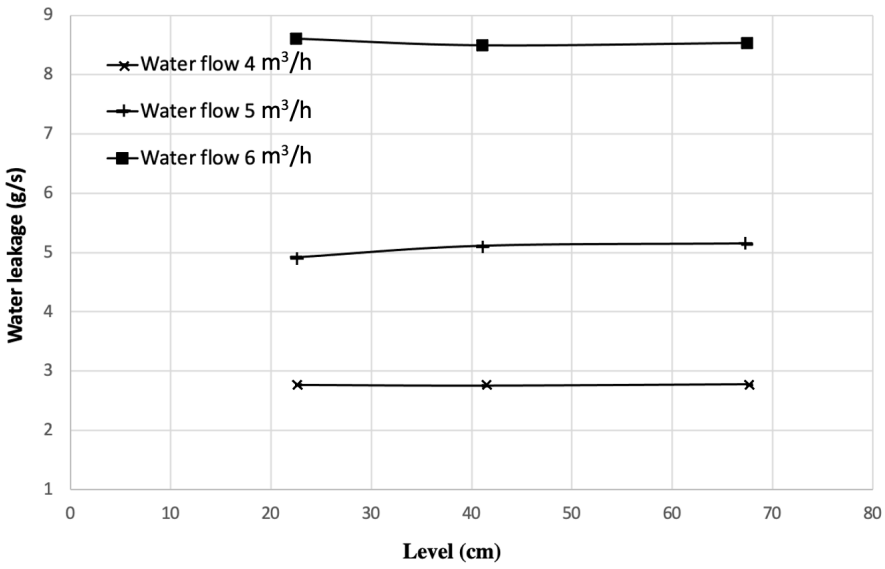

Figure 8: Leakage as a function of level for different water inlet flows ($r_{air/water}$ = 3)

3.2 Results according to the different operating pressure limits to identify anomalies in previous results

The limit imposed on the operating pressure was finally determined to be the cause for the anomalies identified on graph 6 and 7. Further tests were performed by adding this parameter for P_lim from 2 to 4 bar (the maximum pressure the bench can withstand is 5 bar). However, only the lower flow rates, $D_{water-i}$ = 3, 4, 5 and 6 m^3/h, are possible to compare between them due to the physical limit of the bench at higher flow rates.

Figures 9 - 12 show the results for the different flow rates. Each figure is presented with a fixed flow rate at different air/water ratio and pressure limit.

DOI: 10.13009/EUCASS2022-4391

The curves are plotted based on the mean value. The values of the three measurements are indicated as well. It is observed as they are equally distributed on the map around the mean value. The water leakage can have a difference of 0.1 to 3 g/s, this shows the influence of the operational pressure on the water leakage.

Figure 9 shows that for low water flow, even at high air/water ratio and high operational pressure, there is still a negligible leakage. When increasing the water flow rate, we observe a different scenario. Figure 10 shows $D_{water\text{-}i}$ = 4 m^3/h, with P_lim = 2 bar, there is no leakage up to $r_{air/water}$ = 2.5, but with P_lim = 2 bar and 3 bar, from $r_{air/water}$ = 2, there is already a relatively large amount of leakage: about 3.7 g/s and 4.5 g/s respectively. Also, for $D_{water\text{-}i}$ = 5 m^3/h (Fig.11) and for $D_{water\text{-}i}$ = 6 m^3/h (Fig.12). In general, the leakage increases while increasing ratios and increasing operational pressure.

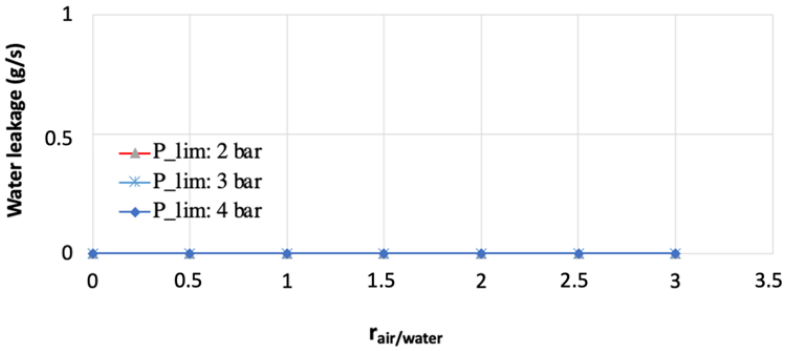

Figure 9: Leakage as a function of ratio for different pressure limits ($D_{water\text{-}i}$ = 3 m^3/h)

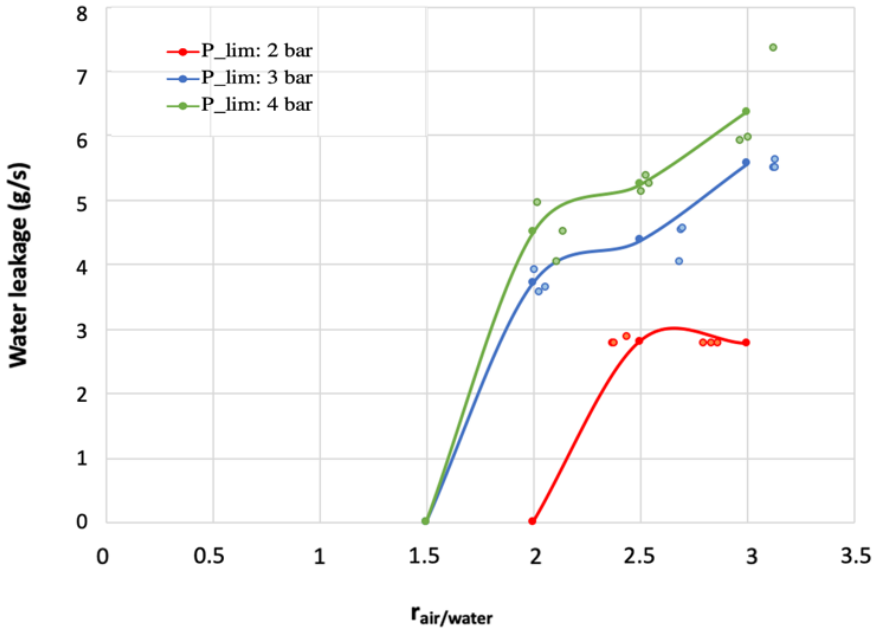

Figure 10: Leakage as a function of ratio for different pressure limits ($D_{water\text{-}i}$ = 4 m^3/h)

DOI: 10.13009/EUCASS2022-4391

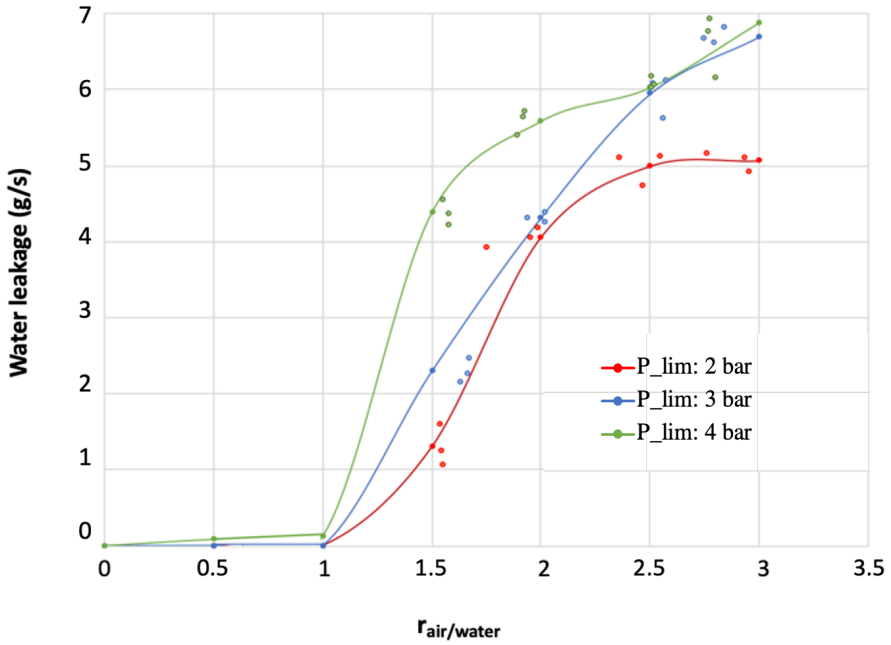

Figure 11: Leakage as a function of ratio for different pressure limits ($D_{water\text{-}i}$ = 5 m^3/h)

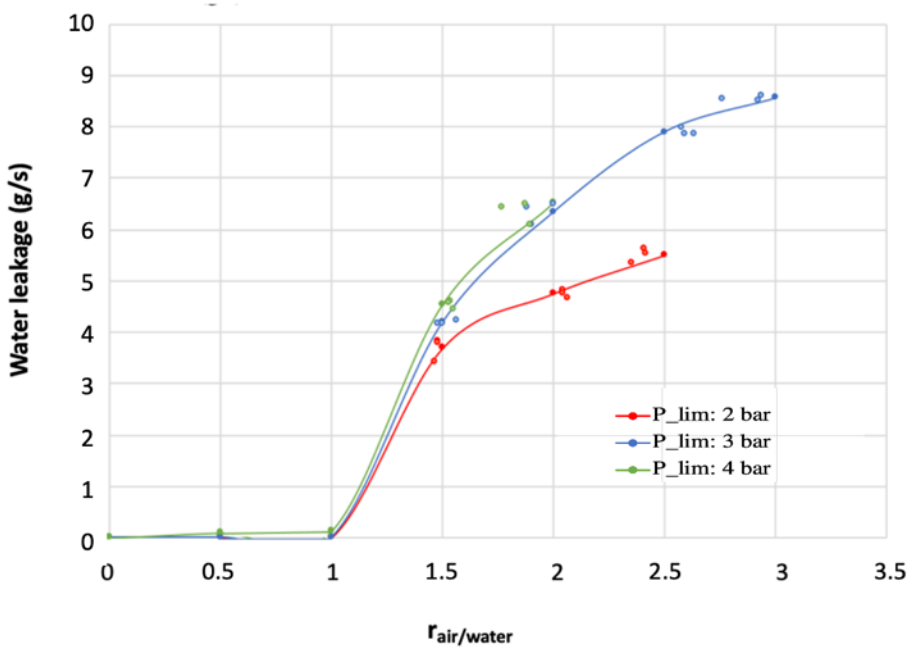

Figure 12: Leakage as a function of ratio for different pressure limits ($D_{water\text{-}i}$ = 6 m^3/h)

The variation of the operational pressure limit impacts the water leakage. However, is observed that the modification of this parameter impact other parameters such as the inlet air pressure and the inlet water pressure. Table 2 shows the variation of the air inlet pressure for the different tested conditions. It is noticed that this value does not vary too much. Therefore, the air pressure inlet is not the determining parameter for the leakage. On the other hand, Table 3 shows the trend of the inlet water pressure $P_{water\text{-}i}$. It is observed an increasing order while increasing P_lim. In this case, the inlet water pressure $P_{water\text{-}i}$ is possibly the parameter that influences the water leakage when changing P_lim. The air/water ratio shows to be an independent parameter; therefore, it remains a parameter that has for sure an impact on the leakage.

DOI: 10.13009/EUCASS2022-4391

Table 2: Air inlet pressure of same conditions $D_{water-i}$ _ $r_{air/water}$ for different P_lim

	4_2[a]	**4_2.5**	**4_3**	**5_0.5**	**5_1**	**5_1.5**	**5_2**	**5_2.5**	**5_3**	**6_0.5**	**6_1**	**6_1.5**	**6_2**	**6_2.5**	**6_3**
P_lim=2 bar	0.7[b]	0.75	0.7	0.61	0.75	0.97	0.64	1.21	1.1	0.62	0.7	1.08	1.15	1.35	LIM
P_lim=3 bar	1.06	1.2	0.71	0.63	0.83	1.02	0.99	1.43	1.66	0.71	0.88	1.07	1.73	1.6	2.6
P_lim=4 bar	1.14	1.06	1.13	0.73	0.82	1.39	1	1.38	1.71	0.78	1.25	1.09	1.87	LIM[c]	LIM

[a]The notation of each column means $D_{water-i}$ (m^3/h)_$r_{air/water}$

[b]Value of air inlet pressure (bar)

[c]Measurement limited by the capacity of the bench

Table 3: Water inlet pressure of same conditions $D_{water-i}$ _ $r_{air/water}$ for different P_lim

	4_2[a]	**4_2.5**	**4_3**	**5_0.5**	**5_1**	**5_1.5**	**5_2**	**5_2.5**	**5_3**	**6_0.5**	**6_1**	**6_1.5**	**6_2**	**6_2.5**	**6_3**
P_lim=2 bar	0.58[b]	0.75	0.7	0.46	0.69	0.77	0.64	1.04	0.99	0.59	0.74	0.93	1.13	1.25	LIM
P_lim=3 bar	0.82	0.89	0.88	0.46	0.69	0.92	0.85	1.19	1.33	0.65	0.87	0.97	1.53	1.93	2.1
P_lim=4 bar	0.95	0.91	1.08	0.56	0.7	1.24	0.94	1.37	1.41	0.71	1.06	1.04	1.76	LIM[c]	LIM

[a]The notation of each column means $D_{water-i}$ (m^3/h)_$r_{air/water}$

[b]Value of water inlet pressure (bar)

[c]Measurement limited by the capacity of the bench

3.3 Results according to the inlet water pressure

The inlet water pressure was previously determined as an influencing factor, so the mappings were made. According to figures 13 - 15, the water leakage increases with the increase of the inlet water pressure $P_{water-i}$. And a predominance on the leakage influence of the inlet water pressure on the ratio air/water is also illustrated: on figure 13 for example, comparing the curves 4_2 and 4_3 (composition $D_{water-i}$ _ $r_{air/water}$), with the same water flow rate, the leakage of $r_{air/water}$ = 2 for P_lim = 3 bar and P_lim = 4 bar are largely higher than the leakage of $r_{air/water}$ = 3 of the P_lim = 2 bar.

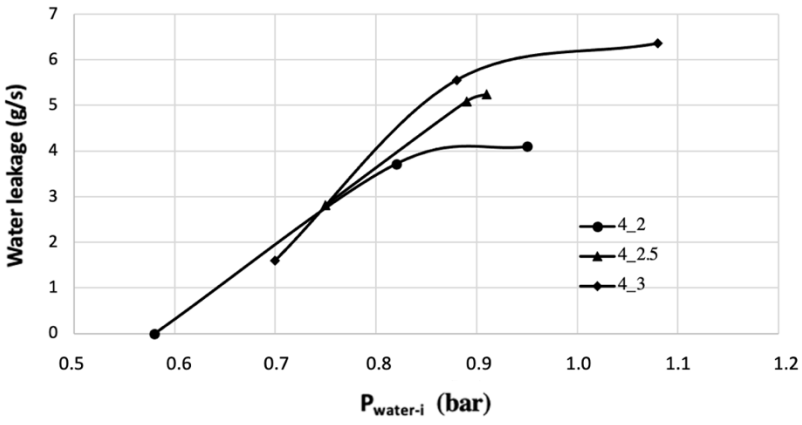

Figure 13: Leakage as a function of different inlet water pressure for different ratios ($D_{water-i}$ = 4 m^3/h)

DOI: 10.13009/EUCASS2022-4391

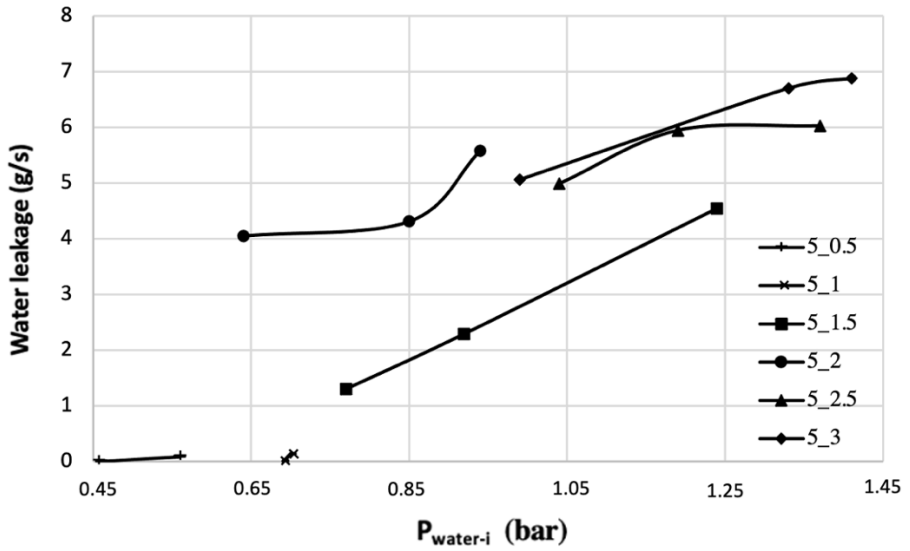

Figure 14: Leakage as a function of different inlet water pressure for different ratios ($D_{water-i}$ = 5m^3/h)

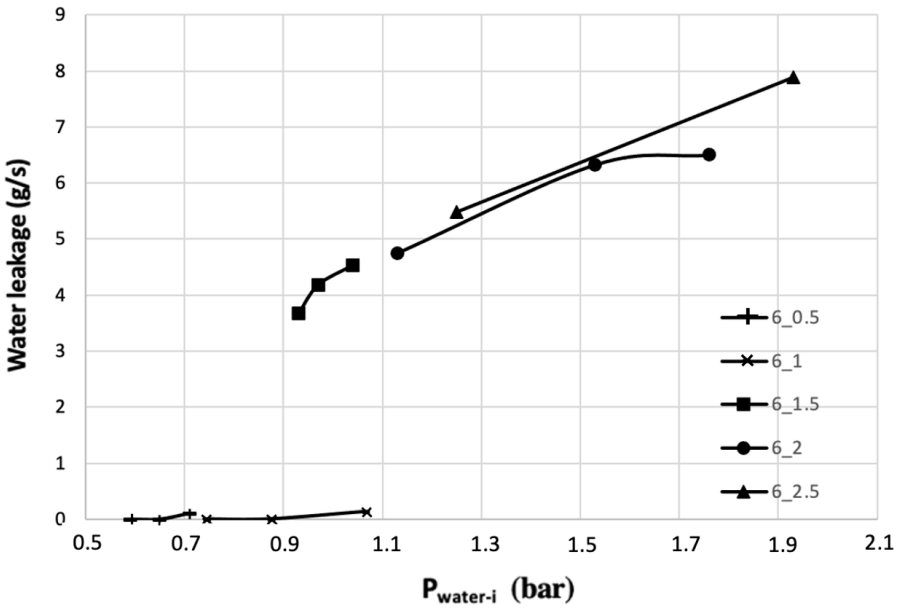

Figure 15: Leakage as a function of different inlet water pressure for different ratios ($D_{water-i}$ = 6m^3/h)

3.4 Results according to air/water volume ratio

The ratio mappings of different pressure limits are also made to see the evolution of the leakage as a function of the ratios for the different flow rates.

Figure 17 shows the result in function of the air/water ratio with fixed P_lim = 3 bar. It is the most complete mapping because it offers the opportunity to explore different combinations of water flow rates and air/water ratio. Nevertheless, can be noted that the curves of the three figures 16 - 18 evolve in the same way: for each flow rate, from a certain ratio, there appears leakage with a rather high slope, then the leakage continues to evolve with the ratio but with a slope of increase smaller and smaller, the curves tend to converge. Except for a high limit pressure (P_lim = 4 bar), with a high ratio and a high water flow rate, the leakage increases strongly. Thus, with the same limiting pressure, for a lower

DOI: 10.13009/EUCASS2022-4391

water flow rate, the leakage will be observed with a higher ratio, for example the case P_lim = 3 bar, for $D_{water\text{-}i}$ = 8 m^3/h and $D_{water\text{-}i}$ = 9 m^3/h, the leakage starts at $r_{air/water}$ = 1, but for $D_{water\text{-}i}$ = 5, 6 and 7 m^3/h, the leakage starts at $r_{air/water}$ = 1.5 and for $D_{water\text{-}i}$ = 4 m^3/h, the leakage starts at $r_{air/water}$ = 2. Furthermore, the slope of the first leakage observed for each water flow rate is increasingly higher with increasing water flow rate (Fig. 17).

Except for low flow rates ($D_{water\text{-}i}$ < = 3 m^3/h), the leakage remains negligible (no measurable by the weighing scale used in this test setup) for any other parameters. It can have $D_{water\text{-}i}$ – $r_{air/water}$ compositions that have very low leakage for every water flow rate and every P_lim. And if water is the only circulating fluid ($r_{air/water}$), the leakage will be negligible even with high inlet water flows (Figs. 16 - 18).

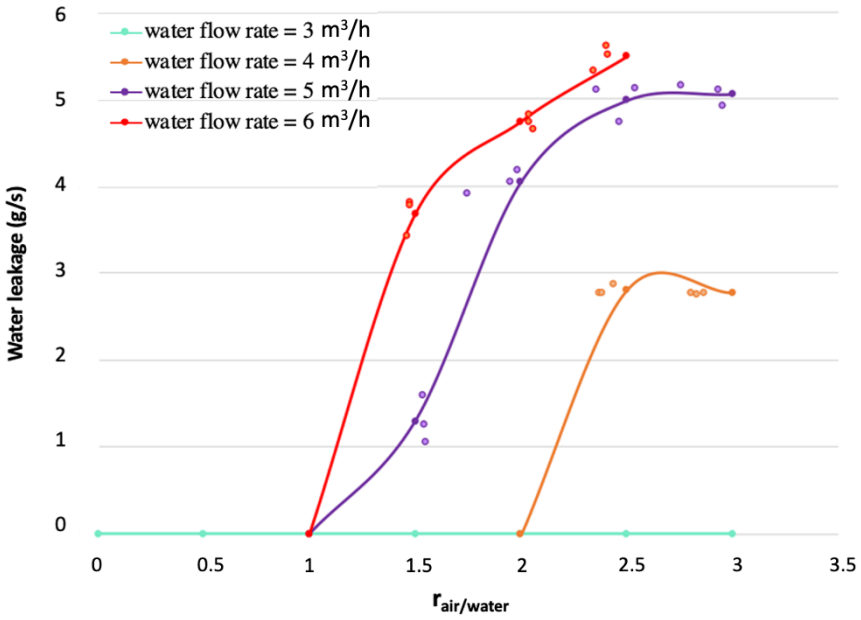

Figure 16: Leakage as a function of ratio for different water flow rates (P_lim = 2 bar)

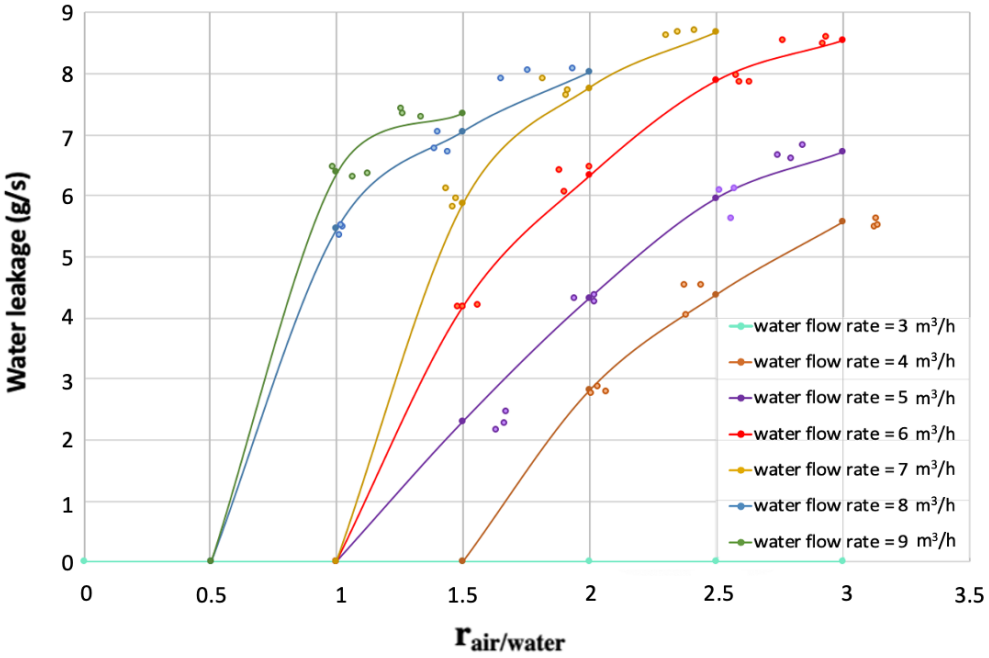

Figure 17: Leakage as a function of ratio for different water flow rates (P_lim = 3 bar)

DOI: 10.13009/EUCASS2022-4391

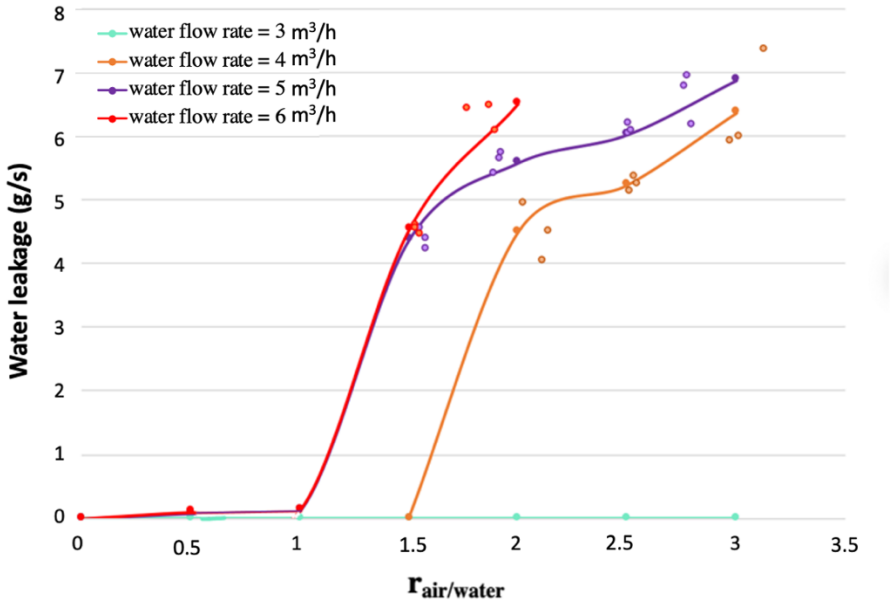

Figure 18: Leakage as a function of ratio for different water flow rates (P_lim = 4 bar)

3.5 Results according to the inlet water flow rate

Figure 19 shows a mapping according to water flow rate and operating pressure at 3 bar for the different air/wate ratio. It better illustrate the evolution of leakage with the water flow rate. Only the one for P_lim = 3 bar has been made because for the other values of P_lim, most of the ratio curves have only 2 or even 1 point which are not representative, only the one for P_lim = 3 bar is more complete and more illustrative.

Figure 19 corresponds to the results analyzed previously; the leakage increases with the increase of the ratio. There is also a tendency to slow down the rate of leakage increase.

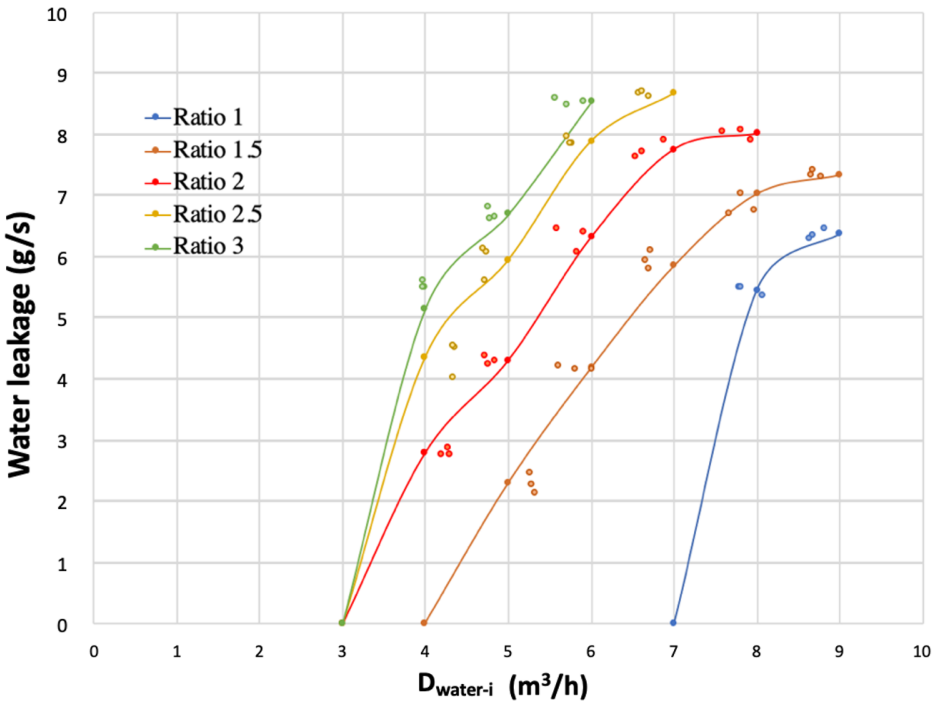

Figure 19: Leakage as a function of water flow for different ratios (P_lim = 3 bar)

DOI: 10.13009/EUCASS2022-4391

4. Conclusions

After having established the maps according to the different operating conditions, the reading of the maps proves the not negligible influence of inlet water flow, air/water volume ratio and inlet water pressure on the water leakage. Therefore, due to the discussed similitude, it may be likely that the same would happen with warm oil and air. The leakage increases with the increase of these parameters and among these three parameters, the inlet water pressure has a predominant impact on the other two, except for the cases of lower flow rates where no measurable leakage is observed despite high air-to-water ratio or high air pressure limits. By managing these parameters, certain operating condition compositions could significantly reduce leakage leading to a much more sustainable impact on the environment.

This analysis opens a new possibility to control oil leakage by managing the operating conditions of the oil/air circuit. The next study and next steps can aim to model the variations with the operating conditions.

References

[1] B. Valkenborgh. 2013.Turbine à gaz. Wallonie Aerotraining network. Part 66 : Module 15.
[2] S. L. K. Wittig, L. Dörr, and S. Kim. 1983. Scaling Effects on Leakage Losses in Labyrinth Seals. *Journal of Engineering for power*. Vol. 105:305-309.
[3] M. Aksit, N. Bhate, C. Bouchard, M. Demiroglu, and Y. Dogu. 2003. Evaluation of brush seal performance for oil sealing applications. In: *39th AIAA/ASME/SAE/ASEE Joint Propulsion Conference and Exhibit.* AIAA-2003-4695.
[4] GCAQE. 2015. Contaminated air overview. GCAQE Global Cabin Air Quality Excutive.
[5] A. Picot, J. Ducret, S. Pasqualini. 2018. Connaissez-vous le Syndrome Aérotoxique ?. ATC Association Toxicologie-Chimie. 1e édition.
[6] C. Winder, and J. -C. Balouet. 2000. Aérotoxic Syndrome: Adverse health effects following exposure to jet oil mist during commercial flights. In: *Proceedings of International Congress on Ocuupational Health Conference*. 196-199.
[7] M. -L. Bossard. 2017. Qualité de l'air dans les avions : substance, concentrations et effets rapporté. Proposition de moyens d'échantillonnage pour une campagne de mesures à grandes échelle, PhD Thesis. Université Claude Bernard – Lyon 1, Faculté de Pharmacie.
[8] C. Winder, and J. -C. Balouet. 2001. Aircrew Exposure to Chemicals in Aircraft: Symptoms of Irritation and Toxicity. *Journal of Occupational Health and Safty*. 471-483.
[9] S. Michaelis, J. Burdon, and C. V. Howard. 2017. Le syndrome aérotoxique: Nouvelles maladie professionnelle?. *Health Panorama*. Vol. 3:198-211.
[10] S. Altmeyer, V. Mathieu, S. Jullemier, P. Contal, N. Midoux, S. Rode, and J.-P. Leclerc. 2004. Comparison of different models of cyclone prediction performance for various operating conditions using a general software. *Chemical Engineering and Processing*. Vol. 43:511–522.
[11] S. Sadighi, M. Shirvani, M. Esmaeli, and R. Farzami. 2006. Improving the Removal Efficiency of Cyclones by Recycle Stream. *Chemical Engineering & Technology*. Vol. 10:1242-1246.
[12] J. Gimbun, T. G. Chuah, Th. S. Y. Choong, and A. Fakhru'l-Razi. 2006. A CFD Study on the Prediction of Cyclone Collection Efficiency. *International Journal for Computational Methods in Engineering Science and Mechanics*. Vol. 6, Issue 3:161-168.
[13] P. Ricco. 2003. Le cœur du SR-71 "Blackbird" : le puissant réacteur J-58. *aerostories*. Partie 2.
[14] M. Milou, J. D. Wurtz and J. Kessous. 2016. Viscosimètre à bille. Département d'enseignement de Physique, Université Montpellier 2.